

# CTQ 839: Candidate for the Smallest Projected Separation Binary Quasar <sup>1</sup>

Nicholas D. Morgan<sup>2</sup>, Greg Burley<sup>3</sup>, Edgardo Costa<sup>4</sup>, José Maza<sup>4,5</sup>, S. E. Persson<sup>3</sup>, Maria Teresa Ruiz<sup>4</sup>, Paul L. Schechter<sup>2</sup>, Ian Thompson<sup>3</sup>, Joshua N. Winn<sup>2</sup>

## ABSTRACT

We report the discovery of the new double quasar CTQ 839. This  $B = 18.3$ , radio quiet quasar pair is separated by  $2''.1$  in  $BRI$  &  $H$  filters with magnitude differences of  $\Delta m_B = 2.5$ ,  $\Delta m_R = \Delta m_I = 1.9$ , and  $\Delta m_H = 2.3$ . Spectral observations reveal both components to be  $z = 2.24$  quasars, with relative redshifts that agree at the  $100 \text{ km s}^{-1}$  level, but exhibit pronounced differences in the equivalent widths of related emission features, as well as an enhancement of blue continuum flux in the brighter component as compared to the fainter component longward of the Ly  $\alpha$  emission feature. In general, similar redshift double quasars can be the result of a physical binary pair, or a single quasar multiply imaged by gravitational lensing. Empirical PSF subtraction of  $R$  and  $H$  band images of CTQ 839 reveal no indication of a lensing galaxy, and place a detection limit of  $R = 22.5$  and  $H = 17.4$  for a third component in the system. For an Einstein-de Sitter cosmology and SIS model, the  $R$  band detection limit constrains the characteristics of any lensing galaxy to  $z_l \gtrsim 1$  with a corresponding luminosity of  $L \gtrsim 5L_*$ , while an analysis based on the redshift

---

<sup>1</sup>Based on observations carried out at the Cerro Tololo Interamerican Observatory (CTIO), the Las Campanas Observatory (LCO), and the National Radio Astronomy Observatory (NRAO) Very Large Array (VLA). CTIO is part of the National Optical Astronomy Observatories, which are operated by the Association of Universities for Research in Astronomy, Inc., under cooperative agreement with the National Science Foundation. The NRAO is a facility of the National Science Foundation operated under cooperative agreement by Associated Universities, Inc.

<sup>2</sup>Department of Physics, Massachusetts Institute of Technology, Cambridge MA 02139; ndmorgan@mit.edu, schech@achernar.mit.edu, jnwinn@mit.edu

<sup>3</sup>Carnegie Observatories, 813 Santa Barbara Street, Pasadena, CA 91101; burley@ociw.edu, persson@ociw.edu, ian@ociw.edu

<sup>4</sup>Departamento de Astronomía, Universidad de Chile, Casilla 36-D, Santiago, Chile; ecosta@das.uchile.cl, jose@das.uchile.cl, mtruiz@das.uchile.cl

<sup>5</sup>Cátedra Presidencial de Ciencias 1996-1998

probability distribution for the lensing galaxy argues against the existence of a  $z_l \gtrsim 1$  lens at the  $2\sigma$  level. A similar analysis for a  $\Lambda$  dominated cosmology, however, does not significantly constrain the existence of any lensing galaxy. The broadband flux differences, spectral dissimilarities, and failure to detect a lensing galaxy make the lensing hypothesis for CTQ 839 unlikely. The similar redshifts of the two components would then argue for a physical quasar binary. At a projected separation of  $8.3 h^{-1}$  kpc ( $\Omega_m = 1$ ), CTQ 839 would be the smallest projected separation binary quasar currently known.

*Subject headings:* gravitational lensing — quasars: individual (CTQ 839)

## 1. INTRODUCTION

The discovery of similar redshift, small separation optical-optical ( $O^2$ ) double quasars (pairs where both components are optically bright and radio faint; see Kochanek, Falco, and Muñoz (1999)) can yield a range of information on cosmological scales. Such systems are intensively investigated as gravitational lens candidates, and if confirmed, can yield measurements of the Hubble constant (Refsdal 1964) as well as statistical constraints on the cosmological constant (Kochanek 1996). If an  $O^2$  pair is confirmed as a binary quasar, it can provide clues regarding the triggering of nuclear activity in galaxies (Osterbrock 1993) as well as the evolution of early ( $z > 2$ ) galaxy mergers (Barnes 1999). The observed frequency of binary quasars are also important in understanding gravitational lensing statistics; Kochanek, Falco, and Muñoz (1999) have recently used the observed paucity of  $O^2R^2$  quasar pairs (pairs with both components bright in optical and radio) as compared to the number of  $O^2$  pairs to conclude that the majority of known wide separation quasar pairs must be binary quasars. In this paper, we report the discovery of the new small separation  $O^2$  quasar pair CTQ 839 and investigate the nature of the system as either a gravitational lens or binary quasar.

CTQ 839 ( $2^{\text{h}} 52^{\text{m}} 57^{\text{s}}.86$ ,  $-32^\circ 49' 8''.6$ , J2000.0) was originally identified as a  $z = 2.24$  quasar from the Calán-Tololo Survey (CTS) (Maza *et al.* 1996). The CTS is an objective prism survey conducted at Cerro Calán using photographic plates obtained at the Cerro Tololo Interamerican Observatory (CTIO) and is aimed at discovering quasars and emission-line galaxies in the southern hemisphere. To date, the CTS has identified  $\sim 1000$  southern hemisphere quasars as well as two confirmed gravitational lenses: CTQ 286 (Claeskens *et al.* 1996) and CTQ 414 (Morgan *et al.* 1999). During November 1998, approximately 100 CTS quasars were observed with the 1.5 m telescope at CTIO as part

of a five night observing program to discover new gravitationally lensed quasars. This particular run has yielded one definite lensed system, the complex gravitational lens HE 0230-2130 (Wisotzki *et al.* 1999), in addition to the double quasar CTQ 839 presented here. Optical images of CTQ 839 immediately revealed two components in the system, with a separation of  $2''.1$  evident in all observed filters. We describe these observations, as well as followup  $R$  and  $H$  band observations conducted at the Las Campanas Observatory (LCO), in §2. In §3, we present our analysis of the quasar components from spectra taken at CTIO, while §4 presents radio observations taken with the Very Large Array (VLA) in July of 1999. In §5 we discuss lens modeling and interpretation of the system, while §6 summarizes our findings and conclusions for CTQ 839.

## 2. OBSERVATIONS AND REDUCTION

### 2.1. Initial Optical Imaging

Initial optical observations of CTQ 839 were taken with the CTIO 1.5 m telescope by two of us (N.D.M. and P.L.S.) on the nights of 1998 November 12 and 15. The SITE 2048 #6 CCD camera was used, although only the central  $1536 \times 1536$  of the array was read out. The telescope was operated at an  $f$  ratio of  $f/13.5$ , providing a field of view of 6.1 arcmin square and a scale of  $0''.2407$  per pixel. The gain and read noise of the detector were  $2.9 \text{ e}^-/\text{ADU}$  and  $4.0 \text{ e}^-$ , respectively. Multiple 300 s exposures of CTQ 839 were taken in Johnson  $B$  and  $R$  and Cousins  $I$  filters with FWHM seeing conditions ranging from  $0''.9$  to  $1''.1$ . Multiple  $BVRI$  exposures of the Landolt standard field Rubin 149 (Landolt 1992) were also taken on the 15<sup>th</sup> for use in photometric calibration. Table 1 presents a log of the CTIO observations. Figure 1 shows a 6 arcmin square exposure of CTQ 839 and nearby stars from one of the  $I$  band frames.

The CCD frames were bias subtracted, trimmed, and flatfield corrected using the Vista reduction program. The flatfield frames consisted of twilight exposures taken on multiple nights of the CTIO observing run, and were cleaned of cosmic rays using “autoclean”, a program written and kindly supplied by J. Tonry. As noted in §1, images of CTQ 839 are separable into two components in all filters (see Figure 2). The double images were therefore fit with two empirical point spread functions (PSFs) using a variant of the program DoPHOT (Schechter *et al.* 1993), designed to deal with close, point-like and extended objects (Schechter and Moore 1993). Star # 5 identified in Figure 1 provided the empirical PSF. Results for the relative positions and apparent magnitudes of the brighter and fainter components (denoted by A and B, respectively) are presented in Table 2. Here we present results from simultaneous fitting of magnitudes and relative positions of the two

components. Magnitude solutions using fixed separations differ by  $< 0.01$  mag in all filters. One of the  $B$  band frames (#54), which registered a cosmic ray detection  $\sim 1''$  north of component B, was omitted from the analysis.

It can be seen that the A:B flux ratio exhibits a rather strong dependence with filter, dropping from  $-2.56$  mag in  $B$  band down to  $-1.85$  mag at  $R$  and  $I$  wavelengths. The  $B$  band separation of  $2''.064$  is also  $\sim 0''.03$  smaller than the separations found at  $R$  and  $I$  wavelengths of  $2''.098$  and  $2''.092$ , respectively. The reason for this difference in image separations at blue and red wavelengths is not immediately clear to us, although we have ruled out variations in the CCD scale as a possible source. Although the separations are consistent with gravitational lensing, the wavelength dependent flux ratio would require strong reddening and/or microlensing of the quasar’s light to conform with the lensing hypothesis. PSF subtraction of components A and B using stacked images for each filter showed no indication of a third component in the system, although deeper and redder searches for possible signs of a lensing galaxy are described in the following subsection.

The observations reported above used the 1.5 m telescope at CTIO operating at a focal length of  $f/13.5$ . The 1.5 m is a Ritchey-Chrétien telescope, designed to be free of comatic aberration at  $f/7.5$ , but not at  $f/13.5$ . Observations were carried out at  $f/13.5$  in order to make use of the smaller pixel scale at that  $f$  ratio. The observations reported above therefore suffer from coma, which introduces an off-axis distortion in the shape of the PSF across the CCD chip. This effect grows with increasing distance from the center of the chip, and, given the relatively good seeing conditions during the observing run, can cause PSF magnitudes to systematically underestimate corresponding aperture magnitudes by as much as 0.1 mag for peripheral stars. In performing the PSF analysis described above, we were careful to choose a PSF star as close as possible to CTQ 839 ( $\sim 30$  arcseconds away) in order to minimize the effects of coma. The resulting PSF and aperture magnitudes for the combined flux from components A and B agree to within 0.035 mag in  $B$ , and better than 0.010 mag in  $R$  and  $I$ .

For use with future observations, aperture magnitudes were determined for 8 field stars within a 4 arcminute radius from the target quasar. An aperture diameter of  $9''.6$  was used. Observations were calibrated using the Rubin 149 standard field (Landolt 1992) mentioned above, with extinction coefficients taken from the 1990 CTIO Facilities Manual ( $k_B = 0.22, k_V = 0.11, k_R = 0.08, k_I = 0.04$ ). These results are presented in Table 3, along with corresponding astrometric solutions for the selected reference stars.

## 2.2. Follow-up Optical and Infrared Imaging

In an effort to further probe the system for the possible presence of a lensing galaxy, follow-up  $R$  and  $H$  band observations were carried out within a few months of the original observations. On 23 December 1998, a series of six 10 minute  $R$  band exposures of CTQ 839 were taken by one of us (E.C.) with the du Pont 2.5 m telescope at LCO. The Tek #5 detector set in the #3 gain position was employed, providing a gain of  $3.0 \text{ e}^-/\text{ADU}$ , a readnoise of  $7.0 \text{ e}^-$ , and scale of  $0''.2604$  per pixel. Seeing conditions for the series of observations were slightly better than those taken at CTIO, with an average FWHM of  $0''.95$ . After bias-subtraction and flatfielding, the images were co-added using integer pixel shifts. The resulting stacked image was then reduced in the same manner as described above. Given the longer exposure times as compared to the CTIO data, star # 5 became saturated on the CCD detector and a new star (# 4 in Figure 1) provided the empirical PSF.

Results from PSF analysis yield an A:B flux ratio of 5.64 and a separation of  $2''.092$  at a PA of  $160^\circ 8$  E of N. Both of these results compare well with the CTIO  $R$  band solutions presented in Table 2. In the two upper panels of Figure 2, we show an excised portion from the stacked image of CTQ 839 (left), along with residuals after PSF subtraction (right). (The bottom two panels show  $H$  band observations taken two months later; see the following subsection). In the residual panels, tick marks indicate the centroid locations of components A and B as determined from the PSF fits. The orientation of the images are the same in all panels of the figure.

When ground-based observations of close separation, doubly lensed systems are fit with two PSFs, a characteristic residual pattern emerges after PSF subtraction. These patterns arise from using only two PSFs to model the light from both quasar images as well as the lensing galaxy, and consist of undulating regions of positive and negative residuals. For instance, one typical residual pattern consists of a “divot-bump-divot” undulation, as seen by Schechter *et al.* (1998) and Morgan *et al.* (1999). These types of patterns are not present in the upper right panel of Figure 2, and therefore argues against the presence of any significant third component in the system. (The residuals located around the center of component A, which do not show significant structure, are likely due to imperfections in component A’s fit). In order to place a magnitude limit on this null result, we inserted a series of gaussian profiles of varying magnitudes into the stacked  $R$  band image and investigated the residual pattern that emerged after fitting each system with two PSFs. The position of the gaussian profile was dictated by the singular isothermal sphere (SIS) model, that is, the center of the gaussian was placed collinear with the centroids of components A and B, with the ratio of relative separations from the two components given by the LCO

$R$  band flux ratio. The FWHM of the profile was dictated by the average seeing conditions for the LCO run. The profile’s magnitude, starting at the same brightness as component B, was successively dimmed by 0.1 mag increments until the characteristic residual pattern was no longer unmistakable. We conclude that we would have confidently detected any third component in the system brighter than  $R = 22.5$  at the expected position for a lensing galaxy.

Following the null result in  $R$  band, infrared observations of CTQ 839 in  $H$  band (1.65 microns) were carried out by two of us (G.B. and I.T.) at LCO on 1999 February 5. The IRCAM infrared camera (Persson *et al.* 1992) mounted on the du Pont 2.5 m telescope was used at a scale of  $0''.3478$  per pixel. The total integration time on CTQ 839 was 3250 seconds, divided into 13 individually dithered frames of  $5 \times 50$  s each. The reduction procedures were carried out by one of us (S.E.P.) and followed closely those described in Persson *et al.* (1998). The 13 fully processed frames were combined into a final stacked image, from which photometry was obtained. Given the narrow ( $256 \times 256$ ) field of view of the detector, only star #5 as shown in Figure 1 was available to provide the empirical PSF. This star is rather bright at  $H = 13.4$ , and as a consequence, the central pixel value for the object required a linearity correction at the 5% level. The residual error associated with this correction affects aperture magnitudes for star #5 no larger than 0.01 mag, which is not critical for the analysis that follows.

Results from empirical PSF analysis yield an  $H$  band A:B flux ratio of 8.42, which is 1.5 times larger than the  $R$  and  $I$  band results. An analysis using an analytical PSF, as described in Schechter *et al.* (1993), yields an A:B flux ratio of 8.30. The  $m_A - m_B$  magnitude differences between the empirical and analytical models therefore differ on the 0.02 mag level. The separation between the two components as determined from empirical PSF fitting was  $2''.101 \pm 0''.020$ , which agrees with the separations found at  $R$  and  $I$  wavelengths. An excised portion of the  $H$  band observation centered CTQ 839, along with residuals after fitting with two empirical PSFs, are shown in the bottom two panels of Figure 2. The residual image again shows no indication of a significant third component in the system. The clustering of positive residuals at the centroid of A’s fit, which are of order 5% of A’s peak intensity, are consistent with the imperfection in the empirical PSF template described above. Using the identical procedure outlined for the LCO  $R$  band data, we conclude that we would have confidently detected a third component at the expected position of a lensing galaxy brighter than  $H = 17.4$ .

### 3. SPECTROSCOPY

Spectra of both components of CTQ 839 were obtained on 1998 December 27 by one of us (M.T.R.) with the 4.0 m telescope at CTIO. The R-C Spectrograph together with the Blue Air Schmidt camera and Loral 3 K  $\times$  1 K CCD were used. The wavelength scale for the observations was 1.205 Å per pixel, with a wavelength range from 3670 to 7210 Å, and a long, 1" wide slit; seeing conditions were 1"3 FWHM. With the slit orientation placed perpendicular to the component separation, one 360 s exposure centered on component A and two 1800 s exposures centered on component B were taken. Three spectrophotometric standard stars from Baldwin and Stone (1984) were also observed during the night for flux calibration purposes. All spectra were bias-subtracted and flatfield corrected using standard IRAF procedures. The observations of CTQ 839 were carried out close to the zenith, with airmasses ranging from 1.001 to 1.010, so differential lightlosses due to atmospheric refraction were not a problem. However, with a separation distance smaller than twice the seeing disc, some contamination of the fainter component's spectra with light from component A was unavoidable. This contamination, which we have estimated to be  $\sim 5\%$  of B's raw spectra, is straightforward to compensate for assuming gaussian profiles and a knowledge of the seeing disc and slit characteristics. In Figure 3, we show the spectra of component A and the decomposed average spectra of component B, along with the identification of prominent emission features.

The spectra of A and B both show quasar emission profiles at similar redshifts. Both components exhibit appropriately redshifted Lyman  $\alpha$   $\lambda$ 1216, N V  $\lambda$ 1240, and C IV  $\lambda$ 1549 emission features, while A also displays O I  $\lambda$ 1304, Si IV  $\lambda$ 1397 + O IV  $\lambda$ 1402, and C III]  $\lambda$ 1909 emission lines as well. Table 4 lists the strongest emission features for both components, as well as redshift determinations based on gaussian fits to the peaks of the profiles. The redshifts of both spectra are consistent with a  $z = 2.24$  quasar. A cross-correlation between the two spectra yields relative redshifts that agree at the 100 km s $^{-1}$  level.

The quotient of the two spectra, shown in Figure 4, shows strong evidence for differences in the equivalent widths of related emission features. The prominent peaks present in the quotient spectrum, corresponding to the C III], C IV, and Ly  $\alpha$ +N V emission features, are consistent with A having progressively stronger emission lines with respect its continuum than B does as one moves from the red to blue wavelengths. There is also an indication for a harder blue continuum in A than in B, longward of the Lyman  $\alpha$  emission feature. As discussed further in §6, these spectral differences between the two components are difficult to reconcile under the lensing hypothesis.

#### 4. RADIO OBSERVATIONS

In order to search for radio emission from CTQ 839, we first queried the NRAO VLA Sky Survey (NVSS) (Condon *et al.* 1998) at the position of the brighter optical component. The NVSS is a 1.4 GHz radio continuum survey of all the sky north of  $-40^\circ$ , carried out with the NRAO Very Large Array (VLA) in its D configuration. The FWHM resolution is 45 arcseconds and the quoted completeness limit is 2.5 mJy. However, no radio source was found within 3 arcminutes of the optical position.

A deeper probe for radio emission from CTQ 839 was performed by one of us (J.N.W.) on 1999 July 21 using the VLA. The search was carried out with a 15 minute integration at 8.4 GHz, while the VLA was in the A configuration. The FWHM of the synthesized beam was 0.5 arcseconds in the N/S direction and 0.2 arcseconds in the E/W direction. No significant sources of radio flux were detected within 5 arcseconds of the position of the brighter optical component of CTQ 839. The rms noise level in this field was 0.17 mJy per synthesized beam, so our observation rules out (at the  $5\sigma$  level) any sources of compact flux above 0.85 mJy. We therefore classify CTQ 839 as an  $O^2$  quasar pair.

#### 5. SIS MODEL AND INTERPRETATION

If CTQ 839 is a gravitational lens system, then the failure to detect a third component can place constraints on the characteristics of any lensing galaxy that may be present <sup>6</sup>. In the following section, we use a simple SIS model to describe the galaxy potential in order to predict the lensing galaxy’s luminosity as a function of distance. Combined with the magnitude detection limits discussed in §2, we investigate the types of bounds that can be placed on the lens galaxy evolutionary type and redshift.

The SIS model is characterized by three parameters: two angular coordinates for the center of the potential, as well as the associated line-of-sight velocity dispersion  $\sigma$  which measures the depth of the potential well. For a SIS model, the velocity dispersion of the lensing potential is related to the image separation  $\theta$  by

$$\frac{\sigma^2}{c^2} = \frac{D_S}{D_{LS}} \frac{\theta}{8\pi} \quad (1)$$

where  $D_S$  and  $D_{LS}$  are angular diameter distances from the observer to the source and from the lens to the source, respectively, and  $\theta$  is measured in radians (see, for example, Narayan

---

<sup>6</sup>In this section, we will continue to refer to the “lensing galaxy”, although we realize its existence is by no means conclusive.



and Bartelmann 1998). We assume the galaxy’s central velocity dispersion is related to its  $B$  band luminosity  $L$  via a Faber-Jackson relationship of the form

$$\frac{L}{L_*} = \left(\frac{\sigma}{\sigma_*}\right)^\gamma, \quad (2)$$

where, following Keeton, Kochanek, and Falco (1998), we adopt  $\sigma_* = 220 \text{ km s}^{-1}$ ,  $\gamma = 4.0$  for early-type galaxies, and  $\sigma_* = 144 \text{ km s}^{-1}$ ,  $\gamma = 2.6$  for late-type galaxies.  $L_*$  corresponds to a  $B$  band magnitude of  $M_B^* = -19.7 + 5 \log h$ , where the Hubble constant has been parameterized by  $H_o = 100h \text{ km s}^{-1} \text{ Mpc}^{-1}$ . For a given redshift  $z_l$  of the lensing galaxy, we can then estimate its cosmological distance modulus via

$$m_{AB}(\lambda_{obs}) - M_{AB}(\lambda_{rest}) = 5 \log \frac{D_L}{10 \text{ pc}} + 7.5 \log(1 + z_l) \quad (3)$$

where  $D_L$  is the angular diameter distance of the lensing galaxy. For the purpose of calculating  $M_{AB}(\lambda_{rest})$ , spectral energy distributions (SEDs) for both early- and late-type galaxies were obtained from Lilly (1997), which consisted of interpolation and extrapolation of the SEDs presented by Coleman, Wu, and Weedman (1980). The SEDs are then normalized to the Faber-Jackson luminosity at  $4400(1 + z) \text{ \AA}$ , which yields the predicted AB magnitudes. Transformations to the  $BVRI$  system from the  $AB$  magnitudes were performed by adding -0.110, 0.011, 0.199, and 0.456, respectively, to the  $AB$  magnitudes (Fukugita, Shimasaku, and Ichikawa 1995).

We have calculated predicted  $R$  band magnitudes for the lensing galaxy as a function of lensing redshift for both an  $\Omega_m = 1, \Omega_\Lambda = 0$  Einstein-de Sitter universe and an  $\Omega_m = 0.3, \Omega_\Lambda = 0.7$  open universe (See Figure 5). For the Einstein-de Sitter cosmology, it can be seen that the late-type spiral model lies above (*i.e.*, brighter than) the detection threshold by a full magnitude for the entire range of  $z_l$ , and makes it therefore an unlikely model for the lensing galaxy. For the same cosmology, the early-type elliptical model requires  $1.0 \lesssim z_l \lesssim 2.0$  for consistency with the detection limit found in §2. At a redshift of  $z_l = 1$ , the elliptical galaxy model is already rather luminous, with an intrinsic luminosity of  $\sim 5L_*$  (corresponding to a velocity dispersion of  $325 \text{ km s}^{-1}$ ). We can estimate the likelihood of finding a lensing galaxy within the above redshift range using the procedures of Kochanek (1992). Using the critical lens radius of  $r = 1''.045$  for CTQ 839, we compute a median redshift for the lensing galaxy of  $z = 0.46$ , with a  $2\sigma$  probability interval of  $0.11 \leq z \leq 0.93$ . Thus, under the lensing hypothesis, the lensing galaxy ought to have been seen in an Einstein-de Sitter cosmology in more than 95% of such cases.

The constraints on the existence of the lensing galaxy are far less stringent for the  $\Lambda$  dominated cosmology. For the  $\Omega_m = 0.3, \Omega_\Lambda = 0.7$  universe, consistency with the  $R$  band

detection limit from §2 requires  $0.7 \lesssim z_l \lesssim 2.1$ . The median redshift is found to be  $z = 0.57$  with a  $2\sigma$  probability range of  $0.16 \leq z \leq 1.07$ , which does not significantly constrain the redshift of the lensing galaxy. Thus while the existence of the lensing galaxy is highly unlikely in an Einstein-de Sitter universe, the  $\Lambda$  dominated model cannot argue for or against the lensing hypothesis.

## 6. SUMMARY AND CONCLUSIONS

Although it may be attractive to explain CTQ 839 as a gravitational lens, there are clearly a number of characteristics of the system that make the lensing hypothesis less than convincing. For example, while the observed image separation of 2.1 is typical of known double gravitational lens systems, the broadband A:B flux ratios (10.4:1 in  $B$ , 5.5:1 in  $R$  and  $I$ , and 8.4:1 in  $H$ ) exhibit a rather large variation with wavelength. Since the detection limit for a third component in the system is  $\sim 22.5$  in  $R$ , the smaller  $R$  and  $I$  band flux ratios is likely not flux augmentation of component B from an intervening galaxy. Also, if this was the case, the SEDs of early-type galaxies would predict an even smaller flux ratio in  $H$  band, which is not observed. Extinction of component B's light by a line of sight absorber is a possible explanation, although such an absorber would have to preferentially absorb more flux at  $B$  and  $H$  wavelengths and less so at  $R$ .

Microensing of quasar light by an intervening galaxy remains a possible explanation for the observed differences in flux ratios, although the situation is highly contrived. First, we note that the quotient spectra shown in Figure 4 exhibits an enhancement of blue continuum flux in component A as compared to component B shortward of the  $\lambda_{obs} \sim 5500\text{\AA}$  mark, which is consistent with microensing of component A's light by stars in an intervening galaxy (Kayser *et al.* 1986). Such an effect has already been observed in at least one confirmed gravitational lens, HE 1104-1805 (Wisotzki *et al.* 1993). However, the observed differences in the line strengths of respective emission features for the two components are difficult to reconcile under the microensing scenario. The line strengths of the emission features, which are thought to arise from a region roughly an order of magnitude larger than the continuum emitting region, ought not to be strongly affected by microensing.

We therefore conclude that CTQ 839 is unlikely to be a gravitationally lensed system. The broadband flux differences, spectral dissimilarities, and failure to detect a lensing galaxy all argue against (although do not explicitly rule out) the gravitational lensing explanation for CTQ 839. If CTQ 839 is not a lens, it must be two separate quasars. The nearly identical redshifts derived from the spectra of the two components would then argue for a physical binary system. At a separation of 2.1 and a redshift of  $z = 2.24$ , the projected

separation of the system is  $8.3 h^{-1}$  kpc ( $\Omega_m = 1$ ), which would make CTQ 839 the smallest projected separation binary quasar currently known (Kochanek *et al.* 1998).

N.D.M. and P.L.S. gratefully acknowledge the support of the U.S. National Science Foundation through grant AST96-16866. J.N.W. thanks the Fannie and John Hertz Foundation for financial support. J.M. thanks FONDECYT, Chile, for support through grant 1980172. M.T.R. acknowledges partial support from FONDECYT, Chile, through grant 19890659 and a Cátedra Presidencial (1996).

## REFERENCES

- Baldwin, J. A., & Stone, R. P. S. 1984, MNRAS, 206, 241
- Barnes, J. E. 1999, in AIP Conf. Proc. *After the Dark Ages: When Galaxies Were Young*, eds. S. S. Holt & E. P. Smith (New York: AIP), 470, 191
- Claeskens, J. -F., Surdej, J., & Remy, M. 1996, A&A, 305, L9
- Coleman, G. D., Wu, C. -C., & Weedman, D. W. 1980, ApJS, 43, 393
- Condon, J. J., Cotton, W. D., Greisen, E. W., Yin, Q. F., Perley, R. A., Taylor, G. B., & Broderick, J. J. 1998, AJ, 115, 1693
- Fukugita, M., Shimasaku, K., & Ichikawa, T. 1995, PASP, 107, 945
- Kayser, R., Refsdal, S., & Stabell, R. 1986, A&A, 166, 36
- Keeton, C. R., Kochanek, C. S., & Falco, E. E. 1998, ApJ, 509, 561
- Kochanek, C. S. 1992, ApJ, 384, 1
- Kochanek, C. S. 1996, ApJ, 466, 638
- Kochanek, C. S., Falco, E. E., Impey, C. D., Lehár, J., McLeod, B. A., & Rix, H., -W. 1998, in AIP Conf. Proc. 470, *After the Dark Ages: When galaxies Were Young*, ed. S. S. Holt & E. P. Smith (New York: AIP), 163
- Kochanek, C. S., Falco, E. E., & Muñoz, J. A. 1999, ApJ, 510, 590
- Landolt, A. U. 1992, AJ, 104, 340
- Lilly, Simon. 1997, Private Communication
- Maza, J., Wischnjewsky, M., & Antezana, R., 1996, R.Mx.A.A., 32, 35
- Morgan, N. D., Dressler, A., Maza, J., Schechter, P. L., & Winn, J. N. 1999, AJ, 118, 1444
- Narayan, R., & Bartlemann, M. 1998, in *Formation of Structure in the Universe*, eds. A. Dekel & J. Ostriker (Cambridge: Cambridge Univ. Press)
- Osterbrock, D. E. 1993, ApJ, 404, 551
- Persson, S. E., West, S. C., Carr, D. M., Sivaramakrishnan, A., & Murphy, D. C. 1992, PASP, 104, 204
- Persson, S. E., Murphy, D. C., Krzeminski, W., Roth, M., & Rieke, M. J. 1998, AJ, 116, 2475
- Refsdal, S., 1964, MNRAS, 128, 307
- Schechter, P. L., Mateo, M., & Saha, A., 1993, PASP, 105, 1342
- Schechter, P. L. & Moore, C. B., 1993, AJ, 105, 1

Schechter, P. L., Gregg, M. D., Becker, R. H., Helfand, D. J., & White, R. L. 1998, *AJ*, 115, 1371

Wisotzki, L., Christlieb, N., Liu, M. C., Maza, J., Morgan, N. D., & Schechter, P. L. 1999, *A&A*, 348, L41

Fig. 1.— a) A 300 s *I* band image of CTQ 839 and the surrounding field taken with the 1.5 m telescope at CTIO. The quasar components are labeled by A (brighter) and B (fainter). Photometric and astrometric solutions for stars labeled 1 through 8 are presented in Table 3. North is up, and east is to the left. The scale is shown in the bottom left of the figure.

Fig. 2.— Excised CCD subrasters centered on CTQ 839 (left) along with residuals after empirical PSF subtractions (right). The top two panels show the stacked *R* band data taken at LCO (summed to  $\sim 60$  min), while the bottom two panels show the  $\sim 54$  min exposure in *H* band. The tickmarks in the two residual panels mark the centroid location of components A and B as determined from empirical PSF fitting. The scale and orientation is identical on all panels, with North up and East to the left. Saturation levels for the residual panels are  $\pm 10\sigma$  where  $\sigma$  is the respective sky noise for each filter, with gray scale intervals every  $1\sigma$ . The peak of component A in *R* (*H*) band is  $\sim 1840\sigma$  ( $\sim 250\sigma$ ).

Fig. 3.— Spectra of the brighter (A) and fainter (B) components of CTQ 839 taken with the 4.0 m at CTIO. Both spectra have been binned by  $6 \text{ \AA}$ .

Fig. 4.— Quotient spectra for CTQ 839, after normalizing at  $6725 \text{ \AA}$ . Bin size is the same as in Figure 3.

Fig. 5.— Predicted *R* band magnitudes for the lensing galaxy as a function of the lens redshift. Two separate cosmologies are considered. The solid and short dashed curves show predictions for an early-type elliptical and late-type spiral, respectively, in an  $\Omega_m = 1, \Omega_\Lambda = 0$  universe. The long dashed curve shows predictions for an early-type elliptical in an  $\Omega_m = 0.3, \Omega_\Lambda = 0.7$  universe. The *R* band detection limit for a third component in the system is indicated by the heavy horizontal line.

Table 1. Log of CTIO Observations (Nov. 1998)

Frame #	Time (UT)	Filter	FWHM (")
052	98 Nov 12 05:49	R	0.88
054	06:00	B	0.99
346	98 Nov 15 05:11	I	1.00
347	05:17	I	1.03
348	05:24	I	1.02
349	05:30	B	1.09
350	05:35	B	1.04
351	05:41	B	0.99
352	05:48	R	0.96

Table 2. Absolute Photometry and Relative Astrometry for CTQ 839

Filter	$N_{im}$	$\Delta$ RA (")	$\Delta$ Dec (")	$m_A$	$m_B$
B	3	$0.644 \pm 0.013$	$-1.961 \pm 0.015$	$18.377 \pm 0.005$	$20.936 \pm 0.030$
R	2	$0.697 \pm 0.009$	$-1.979 \pm 0.002$	$18.086 \pm 0.009$	$19.948 \pm 0.008$
I	3	$0.698 \pm 0.023$	$-1.972 \pm 0.006$	$17.664 \pm 0.009$	$19.517 \pm 0.017$

Note. —  $N_{im}$  is the number of images used in the analysis. Error bars are  $(\sigma^2/N_{im})^{1/2}$  errors from the observed dispersion between the images. Relative coordinates are for component B with respect to component A.



Table 3. Relative Astrometry and Absolute Photometry for Nearby Reference Objects

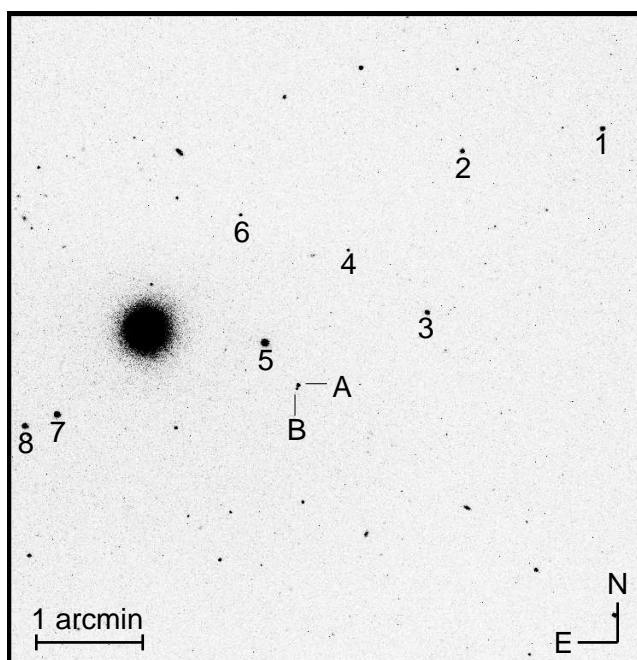
Object	$\Delta\alpha(^{\circ})$	$\Delta\delta(^{\prime\prime})$	$m_B$	$m_R$	$m_I$
1	-15.079	120.82	$20.593 \pm 0.268$	$18.345 \pm 0.023$	$16.942 \pm 0.010$
2	-8.816	108.12	$21.592 \pm 0.104$	$18.586 \pm 0.032$	$17.081 \pm 0.021$
3	-7.252	17.20	$19.751 \pm 0.057$	$18.041 \pm 0.022$	$17.472 \pm 0.004$
4	-3.712	52.20	$20.522 \pm 0.050$	$19.020 \pm 0.049$	$18.538 \pm 0.029$
5	0.000	0.00	$18.456 \pm 0.015$	$15.923 \pm 0.007$	$15.025 \pm 0.003$
6	1.093	72.13	$20.706 \pm 0.146$	$18.992 \pm 0.081$	$18.474 \pm 0.091$
7	9.281	-40.45	$17.955 \pm 0.018$	$16.342 \pm 0.002$	$15.816 \pm 0.005$
8	10.718	-46.98	$19.366 \pm 0.040$	$17.034 \pm 0.009$	$16.308 \pm 0.002$

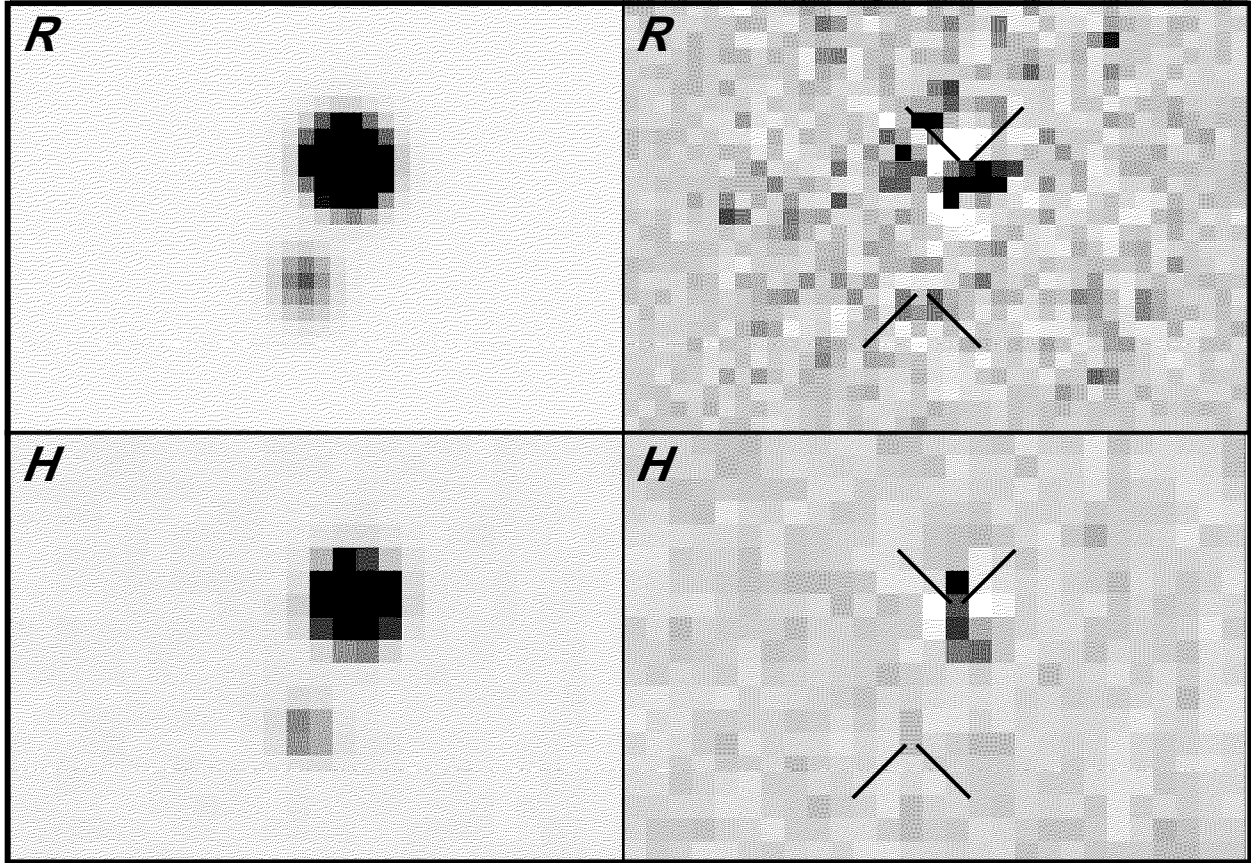
Note. — Magnitudes are from  $9''6$  diameter aperture photometry from the Nov. 1998 CTIO data. Object numbers correspond to the labels shown in Figure 1. Reported error bars are  $(\sigma^2/N_{im})^{1/2}$  errors from the observed dispersion between the images.

Table 4. Redshift Analysis for CTQ 839 A,B

Feature	A		B	
	$\lambda_{obs}$	$z$	$\lambda_{obs}$	$z$
Ly $\alpha$	3943.8	2.244(1)	3950.1	2.249(1)
N V	4020.7	2.240(1)	4018.1	2.238(4)
O I	4228.4	2.244(2)	—	—
C IV	5019.4	2.239(1)	5020.8	2.240(4)
C III]	6187.9	2.242(2)	—	—

Note. — Numbers in parenthesis are  $\pm 1\sigma$  uncertainties in the last digit of the quoted redshift.





# CTQ 839 A and B

